Available online at www.sciencedirect.com
SCIENCE DIRECT®
Journal of Physiology - Paris 96 (2002) 507–516
Journal of Physiology Paris
www.elsevier.com/locate/jphysparis

Multiscale spike train variability in primary electrosensory afferents

Mark E. Nelson*

Beckman Institute for Advanced Science and Technology and Department of Molecular and Integrative Physiology, University of Illinois at Urbana-Champaign, IL 61801, USA

Abstract

Spike train variability is of fundamental importance for understanding how information is encoded and processed in the nervous system. Most studies in this area have focused on short-term variability, as characterized by the coefficient of variation of the interspike interval distribution. Here we discuss the importance of extending the analysis of spike train variability to longer time scales that span multiple interspike intervals. Recent experimental and modeling studies of probability coding (P-type) electrosensory afferent nerve fibers in weakly electric fish have provided new insights into the functional importance of multiscale spike train variability. P-type afferent spike trains are moderately irregular on short time scales of a few milliseconds, but show significantly enhanced regularity on time scales of a few hundred milliseconds. This increased regularity is beyond what would be expected for a renewal process model in which successive intervals are uncorrelated. Modeling studies suggest that the correlation structure that underlies spike train regularization arises from relative refractory effects associated with a dynamic spike threshold. Spike train regularization in P-type afferents has been shown to significantly enhance signal detectability and information transmission on time scales that are functionally relevant for electrolocation behavior.

Keywords: Information transmission; Interspike interval; Sensory coding; Temporal correlations

1. Introduction

Imagine walking into a neurophysiology lab where an audio monitor is broadcasting the sound of single-unit neural activity. The sound of spike activity is unmistakable—not because of the amplitude or the frequency of the activity—but because of the characteristic irregularity of the firing pattern. It is rare to encounter a neuron that fires so regularly that the audio signal takes on the quality of a pure tone or of a metronome. Neuroscientists have pondered and debated the functional importance of spike train variability for decades (for a recent review see [31]). From one perspective it is argued that the variability largely reflects noise in the system and that the nervous system must cope with this intrinsic "sloppiness" of biological neurons. From another perspective it is argued that variability is an essential aspect of neural coding and that increased variability reflects a greater capacity for information transmission. So a key issue to be resolved is the extent to which spike train variability reflects unwanted noise versus the extent to which it reflects a fundamental aspect of the neural code.

Interest in spike train variability has spanned many decades of neurophysiological research. Hagiwara [13] was among the first investigators to take a quantitative approach to the analysis of spike train variability from a statistical viewpoint. The techniques outlined in his seminal paper [13] included analyses of mean, standard deviation, and skewness of the interspike interval (ISI) distributions, the time evolution of the ISI distribution following stimulation, and analysis of serial correlations in the interval sequence. This original paper described experimental work on frog stretch receptors, but Hagiwara also took a similar quantitative approach to analysis of electrosensory afferent spike trains [14–16], which are the focus of this review.

Electrosensory afferents in weakly electric fish have been providing fundamental insights into neural coding ever since their discovery and characterization in the early 1960s. Initial surveys of electrosensory afferent properties across a variety of species established that the nervous system employed a wide diversity of coding

* Tel.: +1-217-244-1371; fax: +1-217-244-5180.
E-mail address: m-nelson@uiuc.edu (M.E. Nelson).

0928-4257/03/$ - see front matter © 2003 Elsevier Ltd. All rights reserved.
doi:10.1016/S0928-4257(03)00006-8

schemes beyond the well-known frequency coding strategy [26]. One such example came from studies of weakly electric fish that exhibit a wave-type electric organ discharge (EOD) waveform. Bullock and Chichibu [4] described two types of novel coding mechanisms that are now referred to as T-type (time coding) and P-type (probability coding), following the terminology of Scheich et al. [30]. Under normal physiological conditions, T-type afferents fire regularly with one spike per EOD cycle and convey timing information. In contrast, P-type afferents fire irregularly and convey information about stimulus intensity. P-type and T-type afferent fibers convey sensory information necessary to support electrolocation and electrocommunication behaviors (for review see [33]).

Present-day studies of electrosensory afferents continue to provide new insights into general principles of sensory coding. This paper will review several recent experimental and modeling studies of P-type afferents, with an emphasis on new insights into the functional role of spike train variability. Many other aspects of P-type afferent response properties have been described previously [2,17,24,34,36]. In reviewing the recent literature, we will describe results from several species of gymnotiform South American wave-type weakly electric fish, including black, brown and glass knifefishes (*Apteronotus albifrons*, *Apteronotus leptorhynchus*, and *Eigenmannia virescens*, respectively). In general, we will not draw distinctions between different species in this review since the mechanisms of sensory coding in P-type afferents appear quite similar.

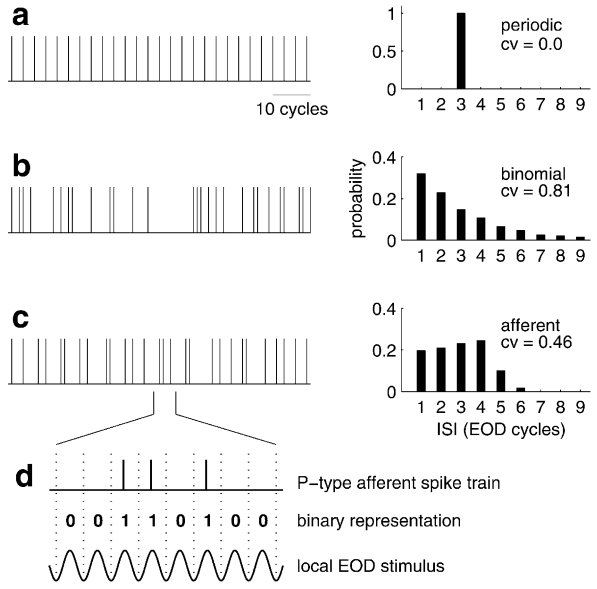

Fig. 1. Representative baseline spike trains and interspike interval histograms (ISIH) for electrosensory P-type afferent models and data. (a) An idealized model in which a spike is generated on exactly every third EOD cycle; the ISIH has a single peak at 3 EOD cycles and a CV of zero. (b) A binomial process model in which the per-cycle firing probability is 1/3; the ISIH has a mean of 3 EOD cycles and a CV of 0.81. (c) Actual P-type afferent data recorded from *A. leptorhynchus* [29]; the ISIH has a mean of 2.9 EOD cycles and a CV of 0.46. The EOD frequency for this unit is 763 Hz. (d) Schematic representation of P-type afferent spike train data as a binary sequence of ones and zeros, based on whether or not a spike was generated on each EOD cycle.

2. P-type afferent response properties

P-type afferents fire irregularly and never fire more than one spike per EOD cycle. EOD frequencies in these fish range from about 200 to 1200 Hz, which means that the period of a single EOD cycle is typically on the order of a few milliseconds. If we ignore the temporal variation within an EOD cycle, the firing pattern can be represented as a sequence of ones and zeros. For example, the activity of a hypothetical P-type afferent that fires on every third EOD cycle would be represented by the binary sequence 100100100..., or equivalently by the interval sequence {3,3,3,...} and would have a mean per-cycle firing probability p of 1/3. The resulting discretized ISI distribution for this sequence would consist of a single peak at 3 EOD cycles and would have a coefficient of variation (CV) equal to zero, where the CV is defined as the standard deviation of the distribution divided by the mean. This hypothetical case of a completely regular firing pattern is illustrated in Fig. 1a. In contrast, if spikes were generated independently with probability 1/3 on each EOD cycle, the ISI pattern would be much more irregular. This case would be described by a binomial process, which can be conceptualized as a sequence of coin tosses with the probability of heads p equal to 1/3. For a binomial process, the probability of observing an interspike interval of j cycles is given by $p(1-p)^{j-1}$ and the CV of the resulting ISI distribution (Fig. 1b) is equal to $\sqrt{1-p}$ [29]. For a probability of 1/3, this corresponds to a CV of about 0.82.

It was realized quite early on [4,15] that P-type afferent spike trains were not completely regular as illustrated in Fig. 1a, nor were they irregular to the extent predicted by the binomial process model as illustrated in Fig. 1b. The variability of P-type afferents falls in between these two extremes, with a typical CV of about 0.5 [19,29]. An ISI distribution from a representative P-type afferent is shown in Fig. 1c and a portion of the corresponding spike train is illustrated in Fig. 1d. This particular unit has a per-cycle firing probability p of 0.34 and a CV of 0.46 (from [29]). Several early studies [4,15,30] speculated that the intermediate degree of variability observed in P-type units might be explained by a relative refractory period following each spike. It turns out that relative refractory effects do indeed play an important role in both short- and long-term spike train variability. We will return to this concept in Section 4, where we discuss computational models of P-type afferents in more detail.

3. Short-term and long-term spike train variability

In neurophysiology, the CV of the ISI distribution is a widely used measure of spike train variability. This definition of variability fits well with our natural intuition. If the spike trains in Fig. 1 were played back over an audio monitor, the perceived degree of irregularity would correlate well with the CV of the ISI distribution. However, there is a limitation to this particular definition of variability. Namely, the CV of the ISI distribution provides information about spike train variability only on short time scales on the order of the mean time between spikes.

There is another aspect of spike train variability that cannot be easily assessed by listening to the spike activity, or by visually inspecting the spike train record, or even by detailed quantitative analysis of the ISI distribution. This more subtle aspect pertains to variability as measured over time scales that span multiple interspike intervals. One approach to analyzing longer-term spike train variability is to extend the idea of ISI analysis to include not only intervals between adjacent spikes, but higher-order intervals as well. This idea is illustrated in Fig. 2, which shows an example of computing the 10th-order interval distribution. The analysis in Fig. 2 is carried out using the same data sets from Fig. 1. The completely regular unit in Fig. 1a, which had a mean ISI of 3 EOD cycles and a CV of zero, gives rise to a 10th-order interval distribution with a mean of 30 EOD cycles and a CV of zero, as shown in Fig. 2a. The binomial process model from Fig. 1b gives rise to a 10th-order distribution, as shown in Fig. 2b. In this case, the mean is 30 EOD cycles and the CV of the 10th-order distribution is 0.26, which is a factor of $\sqrt{10}$ smaller than the CV of the first-order ISI distribution. Finally, in Fig. 2C the P-type afferent fiber gives rise to a 10th-order distribution with a mean of 29 EOD cycles and a CV of only 0.05. This is almost an order of magnitude smaller than the CV of the first-order ISI (0.46). Rather than dropping by a factor of $\sqrt{10}$ as we saw in the binomial case, the CV has dropped by almost a full factor of 10. When spike train variability is assessed over this longer time frame, electrosensory afferents appear much more regular than might otherwise be expected. This unexpected regularity can have important functional consequences.

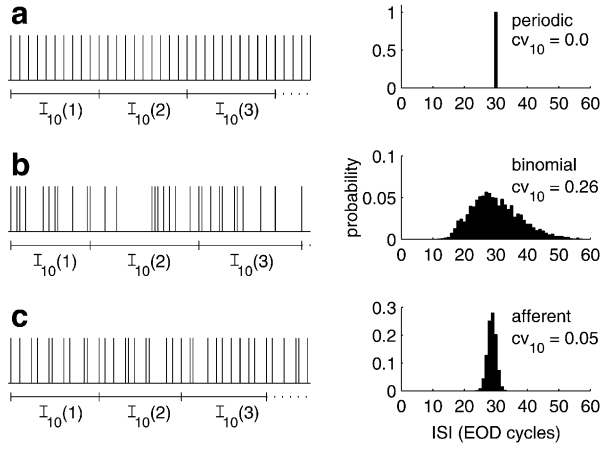

Fig. 2. Computation of higher-order interval distributions. This example illustrates how the 10th-order interval distribution is constructed from the time intervals between every 10th spike in the spike train. The three examples considered here correspond to those shown previously in Fig. 1. (a) An idealized unit that fires on exactly every third EOD cycle gives rise to a 10th order distribution with a single peak at 30 EOD cycles and a CV of zero. (b) A binomial process model with a per-cycle firing probability of 1/3 gives rise to a 10^{th} order distribution with a mean of 30 EOD cycles and a CV of 0.26. (c) The representative P-type afferent spike train from Fig. 1c gives rise to a 10th-order distribution with a mean of 29 EOD cycles and a CV of 0.05. The CV of the 10th-order distribution for this unit is much narrower than would be expected if P-type afferent spike trains were generated by a renewal process.

3.1. Assessing variability on multiple time scales

What is the expected relationship between short-term variability (as reflected by the first-order ISI distribution) and longer-term variability (as reflected by higher-order interval distributions)? It is natural to assume that if spike activity is irregular over the short term, it will also be irregular over the longer term and vice versa. However, the situation is not this straightforward. As a general rule, knowledge of short-term variability does not provide sufficient information to predict longer-term variability of the spike train.

There is one useful case for which a well-defined relationship can be established between short-term and long-term variability. This pertains to a broad class of spike train models called *renewal process* models [8]. In a renewal process, the probability for observing a particular ISI value is independent of previous ISIs in the spike train. That is to say, there are no correlations in the ISI sequence. Furthermore, the underlying process is assumed to be stationary. Under these conditions, the intervals in the spike train are said to be independent and identically distributed. Of course these conditions rarely hold for neurons in the brain, but nevertheless, the renewal process serves as a useful reference for understanding multiscale spike train variability.

For a renewal process model, there is a simple relationship between the mean and variance of the first-order ISI distribution and those of higher-order interval distributions. Consider the example shown in Fig. 3a. If we choose one spike as a reference spike and set the time of this spike to zero, then the mean time to the next spike (averaged over all possible reference spikes) will be equal to the mean of the first-order ISI distribution, which we denote as T. The variance of this first-order ISI distribution will be denoted as σ^2, where the variance is defined as the square of the standard deviation. Now consider the distribution of second-order intervals,

namely the time between the first and third spikes in Fig. 3a. Keep in mind that the first and second intervals are independent and identically distributed. The mean of the second order interval distribution will be sum of the means of the first and second intervals, namely 2T. The variance will be the sum of the variances of the first and second intervals, namely $2\sigma^2$. This argument is readily extended to the kth-order interval distribution, for which the mean will be kT and the variance will be $k\sigma^2$. The key result for a renewal process is that both the mean and variance of the kth-order interval distribution are a factor of k times larger than the mean and variance of the first-order interval distribution.

If there are correlations in the interval sequence or if the underlying process in non-stationary, then the spike generating process is categorized as *non-renewal*. In general, there is no simple relationship between the mean and variance of the first-order and higher-order interval distributions for a non-renewal process. An example of a non-renewal model is illustrated in Fig. 3b. For this particular case, the variance grows more slowly than for the renewal process shown in Fig. 3a. We can tell that this is a non-renewal process because the variance of the kth-order distribution doesn't scale linearly with k, as would be the case for a renewal process.

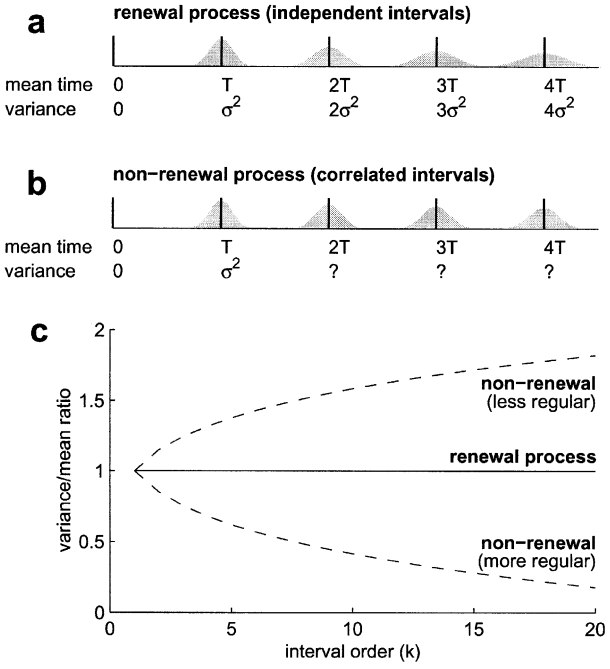

Fig. 3. Mean and variance of the kth-order interval distribution as a function of k. In this example, the first-order ISI distribution is assumed to have a mean of T and a variance of σ^2. (a) For a renewal process model both the mean and variance of the kth-order distribution grow linearly with interval order k. The mean of the kth-order distribution is indicated by a solid vertical line, and the variance is indicated by the spread of the corresponding probability density function (PDF) shown in gray. (b) For a non-renewal model, the mean grows linearly with k, but the variance can grow faster or slower than k, depending on the correlation structure of the spike train. In the example shown here, the variance grows slower than k, as can be seen by comparing corresponding PDFs in (a) and (b). (c) Plotting the variance-to-mean ratio as a function of interval order k provides a convenient assessment of spike train variability on multiple time scales. For a renewal model (solid line), the variance-to-mean ratio remains constant for all interval orders k. For a non-renewal model (dashed lines), the variance-to-mean ratio can increase or decrease depending on whether the process becomes more regular or less regular with increasing interval order.

A convenient way to analyze multiscale variability is to plot the variance-to-mean ratio of the kth-order interval distribution as a function of k. If the spike train data can be explained by an underlying renewal process, then the variance-to-mean ratio will remain constant for all interval orders, as illustrated by the solid line in Fig. 3c. If the spike data arise from a non-renewal process, then the correlations in the interval sequence can act to make the spike train either more or less regular than a renewal process model. If the correlations are regularizing, then the variance-to-mean ratio will decrease with interval order. Conversely if the correlations make the spike train less regular, then the variance-to-mean ratio will increase with interval order. These two possibilities for non-renewal models are illustrated by the dashed lines in Fig. 3c.

3.2. Multiscale spike train variability in P-type afferents

Ratnam and Nelson [29] analyzed the variability of baseline P-type afferent spike activity on multiple time scales using several methods, including an analysis of variance-to-mean ratio as a function of interval order. The results of this analysis for a representative unit are shown in Fig. 4. They found that P-type afferents typically show a pronounced U-shaped variance-to-mean ratio curve, implying that the underlying spike generation process is non-renewal in nature. The variance-to-mean ratio drops quite dramatically for interval orders up to about 50, indicating that the interval correlations are strongly regularizing on this scale. Subsequently the variance-to-mean ratio begins to climb again, eventually crossing the renewal process line for very large interval orders. The minimum in the variance-to-mean ratio in Fig. 4 indicates that spike train regularity is most pronounced for this unit on time scales of about 50–60 interspike intervals, which corresponds to about 200 ms. If the spike intervals are randomly shuffled to remove correlations, then the variance-to-mean ratio remains constant as shown by the open circles in Fig. 4. This serves as a demonstration that two spike trains can have identical first-order ISI distributions, but have very different long-term properties.

Using an ideal observer paradigm, Ratnam and Nelson [29] demonstrated that this form of spike train regularization could significantly improve detection performance for weak signals encoded in P-type afferent spike trains. They illustrated this by comparing the

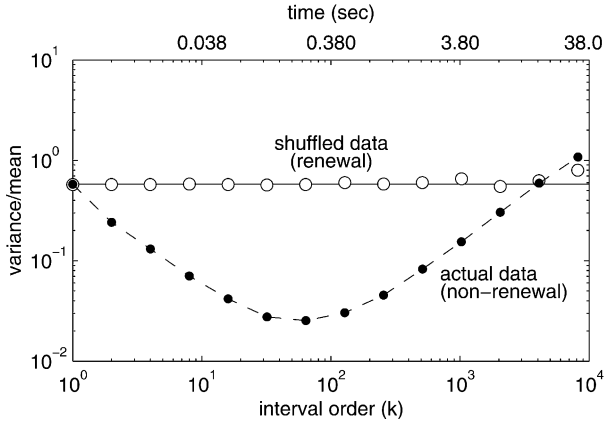

Fig. 4. Variance-to-mean ratio of interval distributions as a function of interval order k for a representative P-type afferent spike train from *A. leptorhynchus* [29]. This is the same unit as in Figs. 1c and 2c. The data (solid circles) show a *U*-shaped dependence on interval order, with a minimum occurring for k on the order of 60 intervals (lower scale), which corresponds to a time scale of approximately 200 ms (upper scale). The decrease in the variance-to-mean ratio is quite pronounced; note the logarithmic scale. When the intervals are randomly shuffled to remove correlations, the shuffled data (open circles) show a variance-to-mean ratio that is independent of interval order k, as expected for a renewal process.

ability to detect extra spikes added to an experimentally recorded spike train versus extra spikes added to a spike train in which the intervals had been shuffled to eliminate correlations. The ability to reliably detect a weak signal depends on being able to distinguish the added signal from transient increases in spike activity due to random fluctuations in background activity. When spike activity is integrated over an appropriate temporal window, spike train regularization dampens the intrinsic fluctuations in background activity making it possible to detect weaker signals. Ratnam and Nelson [29] concluded that P-type afferent spike train regularization permits detection of signals that are a factor of 3–5 times weaker than would otherwise be detectable if spike activity were generated by a renewal process.

3.3. Analysis of spike train variability under non-stationary conditions

Interpreting trends in the variance-to-mean plots is relatively straightforward if the underlying process can be assumed to be stationary, such as under carefully controlled baseline conditions. However, if the spike generating process is being influenced by external time-varying stimuli or if there are other uncontrolled factors influencing the system, then it can become problematic to disentangle the contributions of intrinsic and extrinsic sources of variability.

One approach for dealing with non-stationarity, termed detrended fluctuation analysis (DFA), has been used recently by Bahar et al. [1] to analyze spike train variability in paddlefish electrosensory afferents. The DFA technique was originally developed for the analysis of nonlinear dynamical systems and has been applied, for example, to the analysis of nonstationary heartbeat data [25]. Bahar et al. [1] applied the DFA approach to spike train analysis by first constructing a time series Y_m from the cumulative sum of differences between successive interspike intervals $I(i)$ and the mean interspike interval $\langle ISI \rangle$: $Y_m = \sum_{i=1}^{m} [I(i) - \langle ISI \rangle]$.

The value of Y_m can also be interpreted as the difference between the *actual* time of the mth spike and the *expected* time of the mth spike based on the mean ISI value. Next, the time series Y is divided into non-overlapping windows of equal length n. For each window, a local trend (linear or higher-order) is determined from a least squares fit to Y within the window. This local trend provides a way to account for correlations in the ISI sequence that might arise from slowly varying changes in the stimulus or other environmental factors [25]. A measure of spike train variability $F(n)$ is then defined as the root mean square fluctuations of the detrended time series. This procedure is then repeated for different window lengths to determine how the variability $F(n)$ depends on window length n. If there are no history dependent effects in the spike generating process itself, then $F(n)$ is expected to exhibit a power law behavior of the form $F(n) \propto n^{\alpha}$ with a scaling exponent $\alpha = 1/2$. In other words, the detrended fluctuations are expected to grow as the square root of the window length n. Regularizing effects would give rise to fluctuations that grow more slowly than $\sqrt{n}$ and would thus be revealed as a scaling exponent $\alpha < 1/2$.

Fig. 5 shows an example of detrended fluctuation analysis applied to a representative P-type afferent fiber from a weakly electric fish. The scaling exponent for the afferent data in this case is approximately 0.10, which indicates a strong intrinsic regularizing effect.

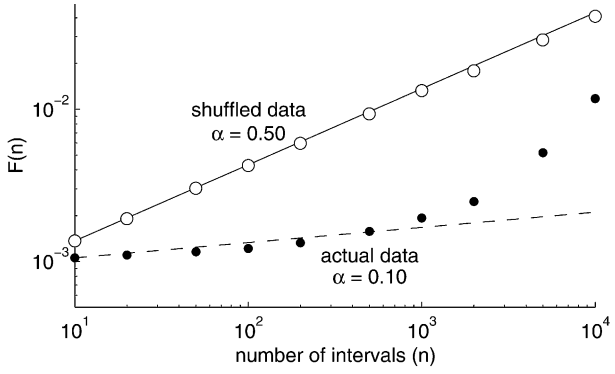

Fig. 5. Detrended fluctuation analysis (DFA) for a representative P-type afferent spike train. This is the same unit that was shown in previous figures. The fluctuation function $F(n)$ is parameterized using a power law relationship of the form $F(n) \propto n^{\alpha}$. The data (filled circles) show a scaling exponent α of approximately 0.10 over the range of 10–1000 intervals, indicating a strong regularizing influence on this time scale. Shuffled data (open circles) show a scaling exponent of 0.5 (i.e., $\sqrt{n}$), as expected for a renewal process with no interval correlations.

For comparison, results are also shown for the same interval sequence after it has been randomly shuffled to remove correlations. The shuffled data show a scaling exponent of 0.5, as expected for an uncorrelated interval sequence. Bahar et al. [1] also observed similar regularizing effects in paddlefish electrosensory afferents. The passive electroreceptor organs of paddlefish are quite different in both structure and function from the P-type electroreceptor organs associated with the active electric sense. Thus the phenomenon of spike train regularization is not just a peculiarity of P-type afferents. This raises the possibility that similar regularizing effects might also exist in other modalities beyond the electric sense.

Detrended fluctuation analysis is most effective when the non-stationary influences are slowly varying. If the stimulus or other external influence is changing rapidly within the analysis window, the trends will not be removed and the measured variability will include contributions from both intrinsic and extrinsic sources. To analyze variability in the presence of rapidly changing external influences other approaches must be utilized. One such approach is to use repeated presentations of a fixed stimulus pattern and then analyze trial-to-trial variability of the resulting spike trains. This approach has been used by Kreiman et al. [19] to analyze the response variability of P-type afferents to time varying stimuli. To analyze the data, trial-to-trial variability was assessed using a spike train distance metric introduced by Victor and Purpura [35]. The distance metric is based on assigning a cost to spike train manipulations that add, delete, or shift the time of a spike. Using this approach Kreiman et al. [19] demonstrated that the short-term timing jitter in P-type afferents in response to time-varying stimuli was on the order of 1–2 EOD cycles. They also quantified the effect of this jitter on information transmission by measuring changes in the coding fraction (for a review see [9,10]) as a function of the amount of added jitter. Interestingly, they found that the degree of short-term jitter observed in P-type afferents did not significantly degrade the amount of information that was being transmitted.

4. Models of P-type afferent spike train variability

Early studies of P-type afferent spike trains led to speculation that relative refractory effects might play an important role in determining the degree of variability observed in these units [4,15,30]. Scheich et al. [30] proposed a conceptual model for P-type afferent spike generation, which is similar to that illustrated in Fig. 6. The EOD is assumed to give rise to an oscillatory membrane voltage that underlies spike generation in the primary afferent fiber. When a spike is generated, the threshold is transiently elevated and decays during the relative refractory period until it once again crosses the oscillatory membrane voltage level and generates the next spike. In the absence of noise, such a model tends to produce a fixed regular interval pattern such as {3,3,3,3,...}, as shown in Fig. 6a, or simple repeating patterns such as {3,3,2,3,3,2,...}. In general, mathematical models of this type can exhibit a variety of stable phase locking ratios depending on the amplitude and frequency of stimulation. The different phase locking regions are referred to as Arnold tongues when represented graphically in the frequency–amplitude plane [11,12]. The ISI sequences from actual P-type afferents exhibit much more variability than would be predicted from these phase-locked patterns, suggesting that some sort of noise process might be involved.

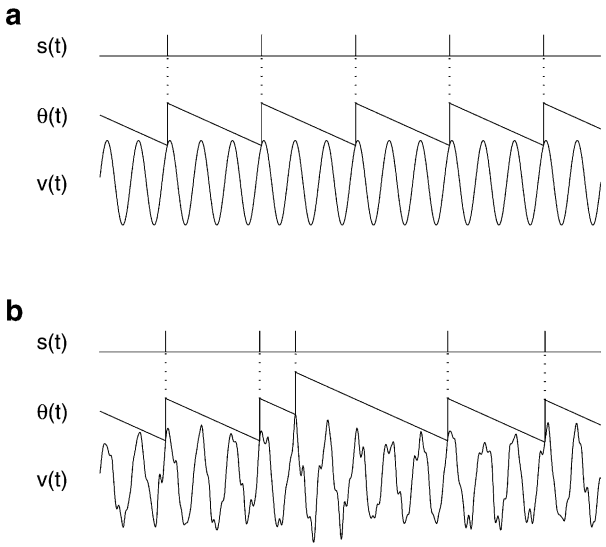

Fig. 6. Conceptual model of P-type afferent spike generation based on a relative refractory mechanism [3,5,7,30]. A spike is generated ($s(t) = 1$) whenever the threshold $\theta(t)$ drops below a voltage level $v(t)$, which is oscillating at the EOD frequency. Immediately following each spike, the threshold level is transiently elevated, giving rise to a relative refractory period. (a) In the absence of noise, spikes are generated with fixed ISI patterns; in this example, the interval pattern is {3,3,3,3} (b) The addition of random voltage fluctuations to the model creates an irregular firing pattern; the interval pattern shown here is {3,1,5,3}. Models of this general form can adequately describe both short-term and long-term spike train variability in P-type afferents.

Scheich et al. [30] collected empirical data describing how the mean ISI varies as a function of electric field intensity. They used their data to estimate how much noise would need to be added to the system in order to explain the observed spread in the ISI distribution. They expressed the noise level in terms of the equivalent fluctuations in electric field intensity that would need to be introduced in the water. The noise level that was necessary to explain the spread of the ISI distribution turned out to be rather large. If voltage fluctuations of this magnitude actually existed in the water around the fish, they would have been easy to detect, but no such fluctuations were observed. Therefore it was hypothesized

that the noise that gives rise to the spread in the ISI distribution is not due to external factors, but is an intrinsic property of the electroreceptor/afferent system. At the time, this conceptual model was not turned into an explicit computational model, but it set the stage for models that would be developed much later by other investigators. Fig. 6b illustrates how adding noise to the membrane voltage signal can introduce variability into the ISI sequence in such a model.

Over the past several years a number of P-type afferent models have been developed. Kashimori et al. [18] presented detailed biophysical models of P- and T-type electroreceptor organs, but did not explicitly address issues of spike train variability. Nelson et al. [24] developed a computational model of P-type afferent dynamics that was used to summarize experimental data on responses to sinusoidal amplitude modulations. A part of this model was devoted to reproducing the intrinsic variability in the ISI distribution. The model consisted of a linear-systems component that described the frequency response characteristics of the afferents, followed by a stochastic spike generating component that converted a continuous representation of the firing rate $r(t)$ into a sequence of spikes. The spike generating portion of this model was purely empirical and was formulated in a manner that allowed a single parameter to control the CV of the ISI distribution. Kreiman et al. [19] developed a similar model to explain their experimental data on multi-trial variability. Their model also incorporated a linear-systems component and a stochastic spike generating mechanism. In this case, spike generation was accomplished by using the firing rate $r(t)$ as the input to an integrate-and-fire mechanism. Rather than using a fixed threshold as is typically done, the integrate-and-fire mechanism used a randomly distributed threshold drawn from a gamma distribution of order n. By adjusting the order of the gamma distribution, the variability of the output spike train could be controlled. Under baseline conditions, both the Nelson et al. [24] model and the Kreiman et al. [19] model give rise to uncorrelated ISI sequences, hence they fall into the category of renewal process models. In both cases, the spike generating mechanism is memoryless. Once a spike is generated, the mechanism is reset and retains no memory of previous spike activity. So while these renewal process models do an excellent job of describing the frequency response characteristics and the short-term variability of P-type afferents, they do not accurately describe longer-term changes in variability that arise from correlations in the ISI sequence.

Chacron et al. [7] developed a model of P-type afferent response dynamics that introduced memory into the spike generating mechanism. Their model for spike generation included a dynamic threshold that was transiently elevated following each spike to give rise to a relative refractory period. They demonstrated that a model similar to that illustrated in Fig. 6b could give rise to an ISI distribution that was consistent with experimental data. Not only could the model reproduce the first-order ISI distribution, it was also able to reproduce correlations between neighboring intervals in the ISI sequence. In general, P-type afferent spike trains show a strong negative correlation between adjacent intervals, meaning that short intervals tend to be followed by long intervals, and vice versa. The dynamic spike threshold provides a memory mechanism such that the probability of generating a spike is dependent on previous spike activity; hence this is a non-renewal model. An extended and more detailed version of this model [5] is able to reproduce the frequency response characteristics of P-type afferents as well as the "*U*-shaped" variance-to-mean ratio dependence for higher-order intervals. Chacron et al. [5] used this model to demonstrate that the correlation structure induced by the refractory mechanism can have a beneficial impact on signal detection and information transmission performance. A further elaboration of the model [6] is able to accurately describe both bursty and non-bursty P-type afferent spike trains.

Brandman and Nelson [3] developed a reduced version of the Chacron et al. [5,7] model. The simplified model, referred to as the linear adaptive threshold model has only three parameters and one state variable. As in the original Chacron et al. [7] model, spike train regularization arises from correlations introduced by relative refractory effects. The simplified model was developed with the goal of providing a minimal description of the dynamics that are necessary for spike train regularization. The model is also computationally efficient; a modified version has been used to simulate afferent activity over the entire population of 15,000 P-type electrosensory afferent nerve fibers during reconstructed prey capture sequences [21]. Because of its simplicity, the model is easily adaptable to other neural modeling applications, beyond the P-type afferent system. When faced with the task of creating a spike train model that includes long-term regularizing effects, this model may provide a useful starting point for developing system-specific models.

Taken together, these modeling studies provide several insights into plausible biophysical mechanisms and functional implications associated with multiscale spike train variability. Four key neural mechanisms seem to be required to reproduce the observed multiscale effects: a leaky integrate-and-fire mechanism for generating spikes in the afferent nerve fiber, a mechanism for generating a relative refractory period following each spike, a fast noise component to introduce short-term variability into the ISI sequence, and a slow noise component to reproduce the upturn in the variance-to-mean plot at long time scales. Interestingly, the time scale at which the minimum occurs in the variance-to-mean ratio curve

is not directly related to the adaptation time scale of the refractory process. Rather, the location of the minimum is largely determined by properties of the slow noise process [5]. From a biophysical perspective, the fast noise is likely to be associated with membrane and synaptic events occurring in the sensory cells of the electroreceptor organ, whereas the slow noise could be due to a wide variety of phenomena either intrinsic to the sense organ, such as drifts in the mean rate of neurotransmitter release from the sensory cells, or extrinsic, such as drifts in the amplitude of the fish's EOD which stimulates those cells.

5. Discussion

One of the key issues introduced at the beginning of this paper was to determine the extent to which spike train variability reflects unwanted noise versus the extent to which it reflects a fundamental aspect of neural coding. Based on what we have learned thus far from P-type afferents, we now know that spike train variability is a multiscale phenomenon. In general, there is no single measure that adequately characterizes the degree of variability across all time scales. Thus the answer to our initial query is likely to depend on the time scale under consideration.

First, we consider the role of spike train variability on short time scales. For P-type afferents, short-term variability is taken to mean something on the order of a few EOD cycles. Remembering that the duration of a single EOD cycle is typically a few milliseconds, this translates into about 3–10 ms. This is the time scale that characterizes the standard deviation of the typical ISI distribution under baseline conditions [29]. This is also the time scale that characterizes the trial-to-trial jitter in individual spike times, based on repeated presentations of a fixed stimulus waveform [19]. Based on both experimental and modeling results, it appears that spike train variability on this time scale is attributable to some sort of intrinsic fast noise process associated with cellular or synaptic events at the level of the electroreceptor/afferent fiber system, rather than with extrinsic source of electrical noise in the environment.

Although it may seem counterintuitive, this intrinsic noise may actually serve to improve overall sensitivity to weak stimuli. Chacron et al. [7] provided one plausible explanation for how noise could potentially improve information transmission in P-type afferents. In the absence of noise, mathematical models predict that neurons driven by periodic stimuli can get locked into fixed spiking patterns, thus making them insensitive to small changes in input [11,27]. Under the right circumstances, additive noise can break up the phase locking pattern, and improve the ability of the system to encode weak signals. Kreiman et al. [19] demonstrated that coding efficiency was not significantly degraded when temporal jitter of 1–2 EOD cycles was artificially added to experimental spike trains. They also speculated that a small amount of temporal jitter would also serve to decorrelate spike trains from neighboring sense organs, thus allowing improvement at the next level of neural processing by averaging across multiple afferents. In summary, short-term variability in P-type afferents is likely to arise from some intrinsic source of random noise that translates into a short-term temporal jitter on the order of 3–10 ms. Rather than degrading performance, short-term spike train variability may actually improve the ability of the system to encode weak signals, both at the single-unit level and at the population level.

Next we consider spike train variability on intermediate time scales of tens to hundreds of milliseconds. This is the time scale on which P-type afferents show a pronounced minimum in the variance-to-mean ratio of kth-order intervals [29]. The time scale on which enhanced regularity is observed appears well matched to the information processing demands placed on the system. For example, this time scale corresponds to the typical duration of electrolocation signals during prey capture behavior [23]. Behavioral studies have shown that small prey such as *Daphnia* can be detected at a distance of about 2 cm from the receptor surface [22]. Based on the physics of electrosensory image formation [28], the electrosensory image of the prey at this distance is a Gaussian-like bump with a full width at half maximum of about 2 cm. During prey capture behavior the fish is typically moving at a velocity of about 10 cm/s relative to the prey. Thus the duration that the electrosensory image of a small prey would activate a single electrosensory afferent fiber is about 200 ms as the image sweeps over the sensory surface. Ratnam and Nelson [29] speculated that spike train regularization on time scales of tens to hundreds of milliseconds plays a key role in enhancing the detectability of these weak sensory signals. Empirical tests, such as detecting single spikes added to experimentally recorded spike trains, as well as more computer modeling studies have shown that spike train regularization can improve detection performance and coding efficiency relative to renewal process models [3,5,29].

Finally we consider long-term variability on time scales of several seconds to minutes. This is the time scale on which P-type afferents show a rapidly rising variance-to-mean ratio for the kth-order interval distributions [29]. This increased irregularity at very long time scales has also been noted in other sensory systems [20,32]. Chacron et al. [5] were able to reproduce this effect in their model by adding a slow random noise component. Thus far there does not appear to be any beneficial role for this long-term irregularity. This would seem to fall into the category of "undesirable"

random noise. However, because this variability appears at long times scales, it may not have much of a negative impact on system performance. We speculate that spike train variability is not tightly controlled by the nervous system once the time scale exceeds the functionally relevant range for neural computation. Increased variability on very long time scales in P-type afferents may thus reflect slow random drift in underlying biological processes, but this drift is unlikely to have a negative impact on the information processing properties of the system.

In summary, recent studies of P-type afferents have highlighted the importance of characterizing spike train variability on multiple time scales. P-type afferents show a dramatic enhancement in regularity on time scales of a few hundred milliseconds. This time scale is well matched to the information processing demands placed on the system during electrolocation behavior. Experimental and modeling studies support the hypothesis that increased regularity arises from the correlation structure of the interval sequence and that these correlations are likely to arise from relative refractory effects associated with a dynamic spike threshold. Given that refractory effects are commonplace in neural systems, we suspect that this form of spike train regularization may be more widespread than previously appreciated. Thus investigators are encouraged to consider the possible implications of multiscale spike train variability in the systems that they study.

Acknowledgements

This work was supported by grants from the National Science Foundation (IBN-0078206) and the National Institute of Mental Health (R01 MH49242).

References

[1] S. Bahar, J.W. Kantelhardt, A. Neiman, H.H.A. Rego, D.F. Russell, L. Wilkens, A. Bunde, F. Moss, Long-range temporal anti-correlations in paddlefish electroreceptors, Europhys. Lett. 56 (2001) 454–460.

[2] J. Bastian, Electrolocation I: How the electroreceptors of *Apteronotus albifrons* code for moving objects and other electrical stimuli, J. Comp. Physiol. A 144 (1981) 465–479.

[3] R. Brandman, M.E. Nelson, A simple model of long-term spike train regularization, Neural Comp. 14 (2002) 1575–1597.

[4] T.H. Bullock, S. Chichibu, Further analysis of sensory coding in electroreceptors of electric fish, Proc. Natl. Acad. Sci. USA 54 (1965) 422–429.

[5] M.J. Chacron, A. Longtin, L. Maler, Negative interspike interval correlations increase the neuronal capacity for encoding time-dependent stimuli, J. Neurosci. 21 (2001) 5328–5343.

[6] M.J. Chacron, A. Longtin, L. Maler, Simple models of bursting and non-bursting P-type electroreceptors, Neurocomputing 38 (2001) 129–139.

[7] M.J. Chacron, A. Longtin, M. St-Hilaire, L. Maler, Suprathreshold stochastic firing dynamics with memory in P-type electroreceptors, Phys. Rev. Lett. 85 (2000) 1576–1579.

[8] D.R. Cox, P.A.W. Lewis, The Statistical Analysis of Series of Events, Methuen, London, 1966.

[9] F. Gabbiani, C. Koch, Principles of spike train analysis, in: C. Koch, I. Segev (Eds.), Methods in Neuronal Modeling: From Ions to Networks, MIT Press, Cambridge MA, 1998, pp. 313–360.

[10] F. Gabbiani, W. Metzner, Encoding and processing of sensory information in neuronal spike trains, J. Exp. Biol. 202 (1999) 1267–1279.

[11] L. Glass, M.C. Mackey, A simple model for phase locking of biological oscillators, J. Math. Biol. 7 (1979) 339–352.

[12] L. Glass, M.C. Mackey, From Clocks to Chaos: The Rhythms of Life, Princeton University Press, Princeton NJ, 1988.

[13] S. Hagiwara, Analysis of interval fluctuation of the sensory nerve impulse, Jpn. J. Physiol. 4 (1954) 234–240.

[14] S. Hagiwara, K. Kusano, K. Negishi, Physiological properties of electroreceptors of some gymnotids, J. Neurophysiol. 25 (1962) 430–449.

[15] S. Hagiwara, H. Morita, Coding mechanisms of electroreceptor fibers in some electric fish, J. Neurophysiol. 26 (1963) 551–567.

[16] S. Hagiwara, T. Szabo, P.S. Enger, Electroreceptor mechanisms in a high-frequency weakly electric fish, *Sternarchus albifrons*, J. Neurophysiol. 28 (1965) 784–799.

[17] C.D. Hopkins, Stimulus filtering and electroreception: tuberous electroreceptors in three species of gymnotid fish, J. Comp. Physiol. A 111 (1976) 171–207.

[18] Y. Kashimori, M. Goto, T. Kambara, Model of P- and T-electroreceptors of weakly electric fish, Biophys. J. 70 (1996) 2513–2526.

[19] G. Kreiman, R. Krahe, W. Metzner, C. Koch, F. Gabbiani, Robustness and variability of neuronal coding by amplitude-sensitive afferents in the weakly electric fish *Eigenmannia*, J. Neurophysiol. 84 (2000) 189–204.

[20] S.B. Lowen, M.C. Teich, Auditory-nerve action-potentials form a non-renewal point process over short as well as long time scales, J. Acoust. Soc. Am. 92 (1992) 803–806.

[21] M.A. MacIver, The Computational Neuroethology of Weakly Electric Fish: Body Modeling, Motion Analysis, and Sensory Signal Estimation, PhD thesis, University of Illinois, Urbana-Champaign, 2001.

[22] M.A. MacIver, N.M. Sharabash, M.E. Nelson, Prey-capture behavior in gymnotid electric fish: motion analysis and effects of water conductivity, J. Exp. Biol. 204 (2001) 543–557.

[23] M.E. Nelson, M.A. MacIver, Prey capture in the weakly electric fish *Apteronotus albifrons*: sensory acquisition strategies and electrosensory consequences, J. Exp. Biol. 202 (1999) 1195–1203.

[24] M.E. Nelson, Z. Xu, J.R. Payne, Characterization and modeling of P-type electrosensory afferent responses to amplitude modulations in a wave-type electric fish, J. Comp. Physiol. A (1997) 532–544.

[25] C.-K. Peng, S. Havlin, H.E. Stanley, A.L. Goldberger, Quantification of scaling exponents and crossover phenomena in nonstationary heartbeat time series, Chaos 5 (1995) 82–87.

[26] D.H. Perkel, T.H. Bullock, Neural coding, Neurosci. Res. Progr. Bull. 6 (1968) 221–348.

[27] D.H. Perkel, J.H. Schulman, T.H. Bullock, G.P. Moore, J.P. Segundo, Pacemaker neurons: effects of regularly spaced synaptic input, Science 145 (1964) 61–63.

[28] B. Rasnow, The effects of simple objects on the electric field of *Apteronotus*, J. Comp. Physiol. A 178 (1996) 397–411.

[29] R. Ratnam, M.E. Nelson, Nonrenewal statistics of electrosensory afferent spike trains: implications for the detection of weak sensory signals, J. Neurosci. 20 (2000) 6672–6683.

[30] H. Scheich, T.H. Bullock, R.H. Hamstra, Coding properties of two classes of afferent nerve fibers: high-frequency electro-

receptors in the electric fish, *Eigenmannia*, J. Neurophysiol. 36 (1973) 39–60.
[31] M.N. Shadlen, W.T. Newsome, Noise, neural codes and cortical organization, Curr. Opin. Neurobiol. 4 (1994) 569–579.
[32] M. Teich, Fractal neuronal firing patterns, in: T. McKenna, J. Davis, S. Zornetzer (Eds.), Single neuron computation, Academic Press, Boston, 1992, pp. 589–625.
[33] R.W. Turner, L. Maler, M. Burrows, Electrolocation and electrocommunication, J. Exp. Biol. 202 (1999) 1167–1458.
[34] R. Wessel, C. Koch, F. Gabbiani, Coding of time-varying electric field amplitude modulations in a wave-type electric fish, J. Neurophysiol. 75 (1996) 2280–2293.
[35] J.D. Victor, K.P. Purpura, Metric-space analysis of spike trains: Theory, algorithms and application, Network-Comp. Neural Syst. 8 (1997) 127–164.
[36] Z. Xu, J.R. Payne, M.E. Nelson, Logarithmic time course of sensory adaptation in electrosensory afferent nerve fibers in a weakly electric fish, J. Neurophysiol. 76 (1996) 2020–2032.